

# Nonconservative forcing and diffusion in refractive optical traps

Ingmar Saberi<sup>†</sup> and Fred Gittes<sup>\*</sup>

*Department of Physics & Astronomy, Washington State University Pullman, WA 99164-2814, USA.* <sup>†</sup>*Present address: Department of Physics, California Institute of Technology, Pasadena, CA 91125, USA.* <sup>\*</sup>*Corresponding author: gittes@wsu.edu*

Refractive optical trapping forces can be nonconservative in the vicinity of a stable equilibrium point even in the absence of radiation pressure. We discuss how nonconservative 3D force fields, in the vicinity of an equilibrium point, reduce to circular forcing in a plane; a simple model of such forcing is the refractive trapping of a sphere by a four rays. We discuss in general the diffusion of an anisotropically trapped, circularly forced particle and obtain its spectrum of motion. Equipartition of potential energy holds even though the nonconservative flow does not follow equipotentials of the trap. We find that the dissipated nonconservative power is proportional to temperature, providing a mechanism for a runaway heating instability in traps.

PACS numbers: 05.60.Cd, 37.10.Vz, 42.50.Wk, 45.10.Na, 05.40.Jc, 42.15.-i, 87.80.Cc

## INTRODUCTION

Nonconservative fields of optical force on optically trapped particles have long been predicted to occur [1]. These force fields are locally nonpotential in character so that net work is done on a particle even in microscopic closed paths. This differs from, say, electromotive force around a circuit where only the global potential is not definable[2]. In a locally nonconservative force field, external power is continuously coupled to particle motion, leading to dissipation and heating even when the particle is localized about a stable point of the force field.

Radiation pressure on trapped particles can be one source of nonconservative forcing. In recent experiments [3, 4] nonconservative toroidal circulation of optically trapped particles caused by axial radiation pressure was observed and theoretically analyzed. Recent theoretical work [5] has shown how, for nonspherical objects, non-conservative motion arises in coordinates of angle and translation.

Here we show that a simple spatial 3D nonconservative force field, circular rather than toroidal, occurs even in the absence of radiation pressure. As a physical model leading to this force, we describe a sphere trapped by refracting rays. Within any such circular-forcing model, and generalizing to an anisotropic trapping force, we derive the spectrum of motion and the thermal signatures of nonconservative circular forcing.

## GEOMETRY OF NONCONSERVATIVE FORCES

Before narrowing the discussion to optical trapping, we ask what simple generic statements can be made about nonconservative forces. Powerful classification schemes are available from differential geometry [6–8] but to use these one must correctly identify forces as fields, not of vectors, but of differential 1-forms. This means that force components such as  $f_x$ ,  $f_y$ , and  $f_z$  properly take their

meaning from the work differential, or work 1-form,

$$\omega = f_x dx + f_y dy + f_z dz \quad (1)$$

which is the integrand for evaluating work along any chosen path. The 1-form  $\omega$  is said to be exact if Eq. (1) equals the differential of some potential function,  $\omega = -d\Phi$ ; otherwise  $\omega$  is inexact. For our purposes an exact 1-form is the same thing as a conservative force.

In Euclidean space one can reinterpret  $f_x$ ,  $f_y$ , and  $f_z$  as components of a vector. But as a 1-form field, Eq. (1) is constrained by Darboux's theorem [6, 7], which states that every 1-form field  $\omega$  can be reduced by some choice of general coordinates  $(q_1, q_2, q_3, \dots)$  to a shortest canonical form  $\omega = \omega^{(k)}$  belonging to the sequence

$$\omega^{(1)} = dq_1, \quad (2)$$

$$\omega^{(2)} = q_1 dq_2, \quad (3)$$

$$\omega^{(3)} = dq_1 + q_2 dq_3 \quad (4)$$

In more than three dimensions the list continues with  $\omega^{(4)} = q_1 dq_2 + q_3 dq_4$ , and so on.

The case  $\omega = \omega^{(1)}$ , i.e.  $\omega = dq_1$ , is exact, i.e. conservative. Not only is  $q_1$  a coordinate, but  $-q_1$  is the potential function for  $\omega$ . The case  $\omega = \omega^{(2)}$ , or  $\omega = q_1 dq_2$ , is reducible to the exact case by an integrating factor  $(1/q_1)$ , since  $(1/q_1)\omega = dq_2$ . In two dimensions this exhausts our list, showing that all 1-forms (i.e., differentials) in 2D are either exact or integrable, a well-known and useful fact in thermodynamics.

In 3D, exact (conservative) and integrable force fields of types  $\omega = \omega^{(1)}$ , and  $\omega = \omega^{(2)}$  can still occur, but the most general possibility is the nonintegrable 1-form  $\omega^{(3)}$ , i.e.  $\omega = dq_1 + q_2 dq_3$ . The form of a generic force field is thus more restricted than Eq. (1) would suggest. In the case of optical trapping, the optical force field includes a part derivable from a potential, which we use for our first coordinate:  $q_1 = -\Phi$ . Following Eq (4), we write

$$\omega = f d\theta - d\Phi \quad (5)$$

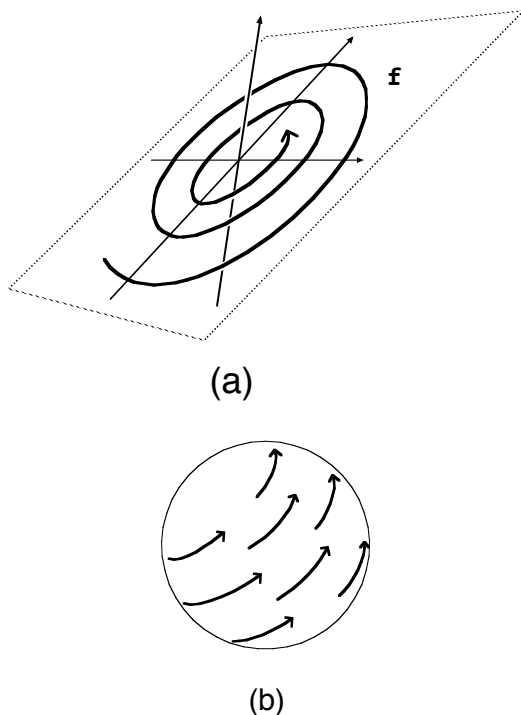


FIG. 1: A nonconservative 3D force field near a stable equilibrium point. The circulation of force may be viewed as purely circular in some plane. (a) Vector flow-field point of view. (b) Combed-hair-on-a-sphere point of view.

so that  $q_3 = \theta$  is a coordinate which we will below take to be an angle, and  $q_2 = f$ , the angular force conjugate to  $\theta$ . The Frobenius theorem [6–8] states that in terms of the exterior product  $\wedge$  and exterior derivative  $d$ , the work 1-form will be of the nonintegrable form of Eq. (5) whenever  $\omega \wedge d\omega = -d\Phi \wedge df \wedge d\theta \neq 0$ .

In the neighborhood of an equilibrium point, where all components of a force field vanish, it is natural to interpret  $\theta$  in Eq. (5) as an angular variable, motivated by the reduction  $-ydx + xdy = \rho^2 d\theta$ . Nonconservative forces near equilibrium are circulations aligned with some plane that contains the equilibrium point. The nonconservative portion of the force can be taken as strictly circular near the equilibrium point in any coordinates, since a noncircular 2D force pattern in  $x$  and  $y$  can be written as

$$-ay dx + bx dy = \frac{1}{2}(a+b)\rho^2 d\theta - \frac{1}{2}(a-b)d(xy) \quad (6)$$

and the last term can be absorbed into  $-d\Phi$ . Thus the work 1-form (6) is actually of the type (5), with  $\theta$  a circular angle in terms of  $x$  and  $y$ .

Thus, to study a nonconservative 3D force about an equilibrium point, it is sufficient to consider a circular pattern of force in some 2D plane containing the equilibrium point.

From another point of view, this picture is consistent with equilibrium-point analysis of a vector field  $\mathbf{f}$ , viewed

as flow towards a fixed point [9] (Fig. 1). Briefly, with coordinates  $q_i$  we have  $f_i \approx M_{ij}\delta q_j$  near the fixed point, defining some real matrix  $M$ . The eigenvalues of  $M$  are roots of a cubic equation with real coefficients, and generically yield one real and two complex conjugate roots whose real parts, together with their eigendirections, correspond here to a conservative force field. The imaginary part of the complex pair of eigenvalues defines circulation in some plane. The eigendirections of  $M$  may be stretched and skewed, corresponding to the non-orthogonal coordinates in (4).

From yet another point of view, any vector field restricted to the surface of a sphere (about the equilibrium point) will circulate about the sphere in a 2D fashion, according to the familiar “combed hair on a sphere” theorem of mathematics [8] (Fig. 1).

### NONCONSERVATIVE TRAPPED-SPHERE MODEL

For a “toy model” realization of a circular nonconservative force we consider an optically trapped sphere much larger than than the wavelength of light, so that geometrical optics applies. In our simplified model we assume no reflections (perhaps due to a graduated-index boundary) and we trap the sphere with only a few rays passing almost centrally through the sphere, so that refraction and trapping force can be calculated in a paraxial-ray approximation. Our model is certainly contrived, but is very simple to analyze. In more realistic situations, whenever there is chirality (handedness) of a system of light rays near an equilibrium point, we still expect some degree of circular nonconservative forcing to occur.

We need only consider rays within the plane of Fig. 2(a), containing the sphere center. In the figure the displacement of the sphere center from the ray is exaggerated. The force of the refracted ray on the sphere due to momentum transfer is

$$\mathbf{f} = -\frac{I_0}{c}(\hat{\mathbf{k}}' - \hat{\mathbf{k}}), \quad (7)$$

where  $I_0$  is the power of the ray and  $\hat{\mathbf{k}}$  and  $\hat{\mathbf{k}}'$  are unit vectors for the original and refracted rays. If  $\Delta\theta$  is the angle between  $\hat{\mathbf{k}}$  and  $\hat{\mathbf{k}}'$ , then

$$\mathbf{f} = -\frac{I_0}{c}[(\cos \Delta\theta - 1)\hat{\mathbf{k}} + (\sin \Delta\theta)\hat{\mathbf{r}}_{\perp}] \quad (8)$$

where  $\hat{\mathbf{r}}_{\perp}$  is the direction of  $\mathbf{r}_{\perp}$  (see Fig. 2(a)). We set  $\sin \Delta\theta \approx \Delta\theta$  and  $\cos \Delta\theta - 1 \approx -\Delta\theta^2/2$ , and use paraxial ray transfer matrices [10] to express  $\Delta\theta$  and  $\mathbf{f}$  in terms of the displacement  $\mathbf{r}$  of the sphere. These matrices act on a vector  $(\Delta\theta, h)$  whose components are the angle with and displacement from the optical axis. If matrices  $F_{\text{in}}$  and  $F_{\text{out}}$  describe refraction at the convex surfaces of our

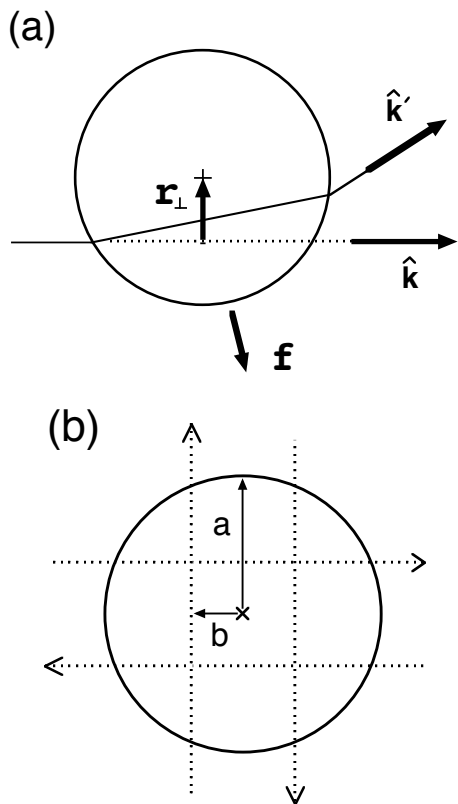


FIG. 2: (a) Refraction of a single ray by a sphere. In the paraxial limit,  $r_{\perp}$  is much smaller than the radius of the sphere. The force  $\mathbf{f}$  acts to return the sphere center to the line of  $\hat{\mathbf{k}}$ , but also has a component along  $\hat{\mathbf{k}}$ . (b) System of four rays for nonconservative trapping. The limit  $b \ll a$  allows a paraxial approximation for each ray.

sphere of radius  $a$ , and matrix  $\mathbf{P}_{2a}$  describes paraxial propagation by a distance  $2a$ , the ray matrix for the sphere is

$$\mathbf{F}_{\text{out}} \mathbf{P}_{2a} \mathbf{F}_{\text{in}} = \frac{2}{n} \begin{bmatrix} 1 - n/2 & -(n-1)/a \\ a & 1 - n/2 \end{bmatrix} \quad (9)$$

with  $n$  the relative refractive index of the sphere. In our case,  $h = -r_{\perp}$  gives

$$\Delta\theta = \frac{2(n-1)}{na} r_{\perp} \quad (10)$$

for the angular deviation. For simplicity we set  $n = 2$  to find

$$\mathbf{f} \approx \frac{I_0}{c} \left[ \frac{r_{\perp}^2}{2a^2} \hat{\mathbf{k}} - \frac{\mathbf{r}_{\perp}}{a} \right]. \quad (11)$$

Eq. (11) resolves  $\mathbf{f}$  into a conservative restoring force, proportional to  $-\mathbf{r}_{\perp}$ , and a nonconservative quadratic force, pushing the sphere along the ray direction  $\hat{\mathbf{k}}$  whenever the sphere center is displaced off the ray axis.

The system of four rays shown in Fig. 2(b) results in a purely circular nonconservative force on the sphere. Despite the clockwise circulation of rays, there is no torque

on the sphere within this ray-optical model: it is the nonconservative net force on the sphere that we study here. We separate oppositely directed ray pairs by a distance  $2b$ , exaggerated in the figure, with  $b \ll a$  so that our paraxial analysis remains valid. The ray in the  $+x$  direction is described by

$$\hat{\mathbf{k}} = \hat{\mathbf{x}}, \quad \mathbf{r}_{\perp} = (y-b)\hat{\mathbf{y}} + z\hat{\mathbf{z}} \quad (12)$$

and similarly for the other rays. Summing the forces from Eq. (11), the total force on the sphere is

$$\mathbf{f} = \frac{2I_0}{ca} \left[ \frac{b}{a} (x\hat{\mathbf{y}} - y\hat{\mathbf{x}}) - (x\hat{\mathbf{x}} + y\hat{\mathbf{y}} + 2z\hat{\mathbf{z}}) \right]. \quad (13)$$

The work differential, or work 1-form, is

$$\omega = \frac{2bI_0}{ca^2} \rho d\theta - d \left[ \frac{I_0}{ca} (x^2 + y^2 + 2z^2) \right] \quad (14)$$

which is of the form of Eq. (5),  $\omega = f d\theta - d\Phi$ .

### NONCONSERVATIVE MOTION OF A DIFFUSING PARTICLE

To look for spectral features of trapping in a nonconservative field, we consider diffusion through a fluid of a particle with drag coefficient  $\gamma$ . At temperature  $T$ , the diffusion coefficient is  $\gamma/k_B T$ , an Einstein relation [11]. Near an equilibrium point we consider 2D motion  $\mathbf{r}(t)$  in a plane of circulation where the nonconservative component of force is

$$\mathbf{f} = \xi \hat{\mathbf{z}} \times \mathbf{r} = \xi \rho \hat{\theta} \quad (15)$$

where  $\xi$ , the strength of the circular forcing, has units of force per distance. As a 1-form,

$$\omega = \xi \rho d\theta. \quad (16)$$

First we check that there is no pathology regarding work done by the nonconservative force at small length scales, where a diffusing particle executes spatial cycles with a diverging frequency. For this, imagine the particle constrained to move on a circle of radius  $\epsilon$ , like a bead sliding on a circular wire. In the absence of the external force, the time to diffuse around the circle is  $\delta t \sim (\gamma/k_B T) \epsilon^2$ . In the presence of a nonconservative force, the rates of positive and negative circling are enhanced and suppressed according to

$$\nu_{\pm} \sim \frac{k_B T}{\gamma \epsilon^2} \exp \left( \pm \frac{\Delta W}{k_B T} \right) \quad (17)$$

where  $\Delta W$  is the work done by the nonconservative force in a “+” cycle; for our force this is  $\Delta W = 2\pi \epsilon f \sim \xi \epsilon^2$ . The net “+” rate is  $\Delta \nu = \nu_+ - \nu_- \sim \Delta W / \gamma \epsilon^2$ , implying that the dissipated power is

$$\Delta \nu \Delta W \sim \frac{\xi^2 \epsilon^2}{\gamma}. \quad (18)$$

We conclude that the power supplied by the nonconservative force vanishes at small scales, as the square of the spatial scale of the motion.

We turn to the spectral properties of the diffusing particle, and first establish formalism [13] with force and motion only in the  $x$  direction. For a force  $f(t)$  and motion  $x(t)$  that extend over all time, the spectral density  $(fx)_\omega$  is defined by [12]

$$\langle f_\omega x_{\omega'}^* \rangle = 2\pi (fx)_\omega \delta(\omega - \omega') \quad (19)$$

where  $f_\omega$  and  $x_\omega$  are Fourier transforms of functions truncated outside of a time  $T$ . Throughout,  $(\dots)_\omega$  specifies a spectral density, whereas  $\langle \dots \rangle$  is an average. Standard manipulations [12], or more simply the formal replacement  $\langle f_\omega x_{\omega'}^* \rangle = T (fx)_\omega$ , give the rate of work done by  $f$  as

$$\left\langle \frac{dW}{dt} \right\rangle = \frac{1}{2\pi} \int (fv)_\omega d\omega = \frac{1}{2\pi} \int i\omega (fx)_\omega d\omega. \quad (20)$$

Spectral densities integrate to correlations or mean squared fluctuations [12] In the 1D case, if a thermal Nyquist force  $N(t)$  acts on the object, with  $(N^2)_\omega = 2\gamma k_B T$  (with  $\gamma$  the drag coefficient) then in an external conservative force  $f = -\kappa_x x$ , with  $\alpha_x = \kappa_x/\gamma$ , the equation of motion  $N = \kappa_x x + \gamma \dot{x}$  gives us

$$N_\omega = -i\gamma(\omega + i\alpha_x)x_\omega \quad (21)$$

$$\langle N_\omega N_{\omega'}^* \rangle = \gamma^2(\alpha_x^2 + \omega^2)\langle x_\omega x_{\omega'}^* \rangle \quad (22)$$

The replacements  $\langle N_\omega N_{\omega'}^* \rangle = T(N^2)_\omega$  and  $\langle x_\omega x_{\omega'}^* \rangle = T(x^2)_\omega$  immediately lead to

$$(x^2)_\omega = \frac{2k_B T/\gamma}{\alpha_x^2 + \omega^2}. \quad (23)$$

This Lorentzian spectrum integrates to

$$\langle x^2 \rangle = \frac{1}{2\pi} \int (x^2)_\omega d\omega = \frac{k_B T}{\kappa_x} \quad (24)$$

as it should by the equipartition theorem [13]. Since  $(fx)_\omega = -\kappa_x(x^2)_\omega$  is an even function of  $\omega$ , the rate of external work vanishes.

Now include a circular external force. With an isotropic conservative force  $-\kappa \mathbf{r}$ , the vector equation of motion  $\mathbf{N} = \kappa \mathbf{r} - \xi \hat{\mathbf{z}} \times \mathbf{r} + \gamma \dot{\mathbf{r}}$  gives us

$$\mathbf{N}_\omega = (\alpha - i\omega - \eta \hat{\mathbf{z}} \times) \mathbf{r}_\omega \quad (25)$$

with “ $\times$ ” a cross product, and where  $\alpha = \kappa/\gamma$ , and  $\eta = \xi/\gamma$ . In the absence of thermal forces, the particle spirals to the origin with angular frequency  $\eta$  and a radius proportional to  $\exp(-\alpha t)$ , similar to Fig. 1(a). Using the column vectors

$$\mathbf{N}_\omega = \begin{bmatrix} N_{x,\omega} \\ N_{y,\omega} \end{bmatrix}, \quad \mathbf{r}_\omega = \begin{bmatrix} x_\omega \\ y_\omega \end{bmatrix} \quad (26)$$

we can analyze an anisotropic confining potential, with Eq. (21) generalized to

$$\mathbf{N}_\omega = -i\gamma \mathbf{M} \mathbf{r}_\omega, \quad \mathbf{M} = \begin{bmatrix} \omega + i\alpha_x & i\eta \\ -i\eta & \omega + i\alpha_y \end{bmatrix} \quad (27)$$

and  $\alpha_y = \kappa_y/\gamma$ . To find the power spectrum we form the averaged product

$$\langle \mathbf{N}_\omega \mathbf{N}_\omega^\dagger \rangle = \gamma^2 \mathbf{M} \langle \mathbf{r}_\omega \mathbf{r}_\omega^\dagger \rangle \mathbf{M}^\dagger, \quad (28)$$

a generalization of Eq. (22). In terms of spectral densities we have

$$2\gamma k_B T \mathbf{1} = \gamma^2 \mathbf{M} \langle \mathbf{r} \mathbf{r}^\dagger \rangle_\omega \mathbf{M}^\dagger \quad (29)$$

where  $\mathbf{1}$  is the identity matrix, and the spectral density matrix is

$$\langle \mathbf{r} \mathbf{r}^\dagger \rangle_\omega = \begin{bmatrix} (x^2)_\omega & (xy)_\omega \\ (yx)_\omega & (y^2)_\omega \end{bmatrix}. \quad (30)$$

Eq. (29) is easily solved for  $\langle \mathbf{r} \mathbf{r}^\dagger \rangle_\omega$ , giving diagonal elements

$$(x^2)_\omega = \frac{2k_B T}{\gamma} \frac{\omega^2 + \alpha_y^2 + \eta^2}{[\omega^4 + (\alpha_x^2 + \alpha_y^2 - 2\eta^2)\omega^2 + (\eta^2 + \alpha_x \alpha_y)^2]} \quad (31)$$

which generalizes Eq. (23);  $(y^2)_\omega$  is the same with  $\alpha_x$  and  $\alpha_y$  interchanged.

Eq. (31) represents the power spectrum of  $x$ -motion of a trapped particle with a nonconservative force ( $\eta \neq 0$ ) and 2D anisotropy ( $\alpha_x \neq \alpha_y$ ) both in the  $xy$  plane. Nonconservative forces make this power spectrum non-Lorentzian even in an isotropic trap. Other interesting effects such as inertial hydrodynamics and material properties [14, 15] will of course also invalidate a simple Lorentzian spectrum. Carrying out the  $\omega$  integral in Eq. (24), we obtain

$$\langle x^2 \rangle = \frac{k_B T}{\kappa_x + \kappa_y} \left[ 1 + \frac{\xi^2 + \kappa_y^2}{\xi^2 + \kappa_x \kappa_y} \right]. \quad (32)$$

For  $\langle y^2 \rangle$ ,  $\kappa_x$  and  $\kappa_y$  are interchanged. In the isotropic case,  $\kappa_x = \kappa_y = \kappa$ , the nonconservative circulation preserves  $\langle x^2 \rangle = k_B T/\kappa$ . For large values of  $\xi$ ,

$$\langle x^2 \rangle = \frac{2k_B T}{\kappa_x + \kappa_y}, \quad \xi \gg \kappa_x, \kappa_y \quad (33)$$

and the potential is effectively being averaged by rapid circulation. However, for all values of  $\xi$ ,  $\kappa_x$ , and  $\kappa_y$  we find

$$\left\langle \frac{1}{2} \kappa_x x^2 + \frac{1}{2} \kappa_y y^2 \right\rangle = k_B T \quad (34)$$

so that the equipartition of potential energy is unaffected by nonconservative circulation, even though the nonconservative flows do not follow equipotentials in an anisotropic trap.

Details of the flow pattern follow from the off-diagonal element of  $(\mathbf{r}\mathbf{r}^\dagger)_\omega$ ,

$$(xy)_\omega = \frac{2k_B T}{\gamma} \frac{\eta(\alpha_y - \alpha_x) - 2i\eta\omega}{[\omega^4 + (\alpha_x^2 + \alpha_y^2 - 2\eta^2)\omega^2 + (\eta^2 + \alpha_x\alpha_y)^2]} \quad (35)$$

obtained by solving Eq. (29). Integrating this over  $\omega$  yields

$$\langle xy \rangle = \frac{k_B T}{\kappa_x + \kappa_y} \frac{\xi(\kappa_y - \kappa_x)}{\xi^2 + \kappa_x \kappa_y} \quad (36)$$

Using this result we can generalize Eq. (32) to mean squared radius at any 2D angle. For Gaussian statistics such as we have here, the probability distribution

$$P(x, y) \propto \exp[-\frac{1}{2}\mathbf{r}^\top \mathbf{G} \mathbf{r}] \quad (37)$$

yields a matrix of averages  $\langle \mathbf{r}\mathbf{r}^\top \rangle = \mathbf{G}^{-1}$ , and a unit ellipse defined by

$$\mathbf{r}^\top \mathbf{G} \mathbf{r} = \mathbf{r}^\top \langle \mathbf{r}\mathbf{r}^\top \rangle^{-1} \mathbf{r} = 1. \quad (38)$$

As a function of angular direction  $\theta$ , the squared radius of the ellipse is

$$r^2 = \frac{\langle x^2 \rangle \langle y^2 \rangle - \langle xy \rangle^2}{\langle y^2 \rangle \cos^2 \theta - 2\langle xy \rangle \cos \theta \sin \theta + \langle x^2 \rangle \sin^2 \theta} \quad (39)$$

into which  $\langle x^2 \rangle$ ,  $\langle y^2 \rangle$ , and  $\langle xy \rangle$  can be inserted from Eqs. (32) and (36). The resulting ellipses are plotted in Fig. 3 for various values of  $\xi$ . The r.m.s. radius drawn in the figure is necessarily a line of flow. For increasing  $\xi$  the flow pattern does not follow the  $\xi = 0$  equipotential lines, but tilts by  $\theta_\xi$  in the direction of the circular forcing, with

$$\tan 2\theta_\xi = \frac{2\xi}{(\kappa_x + \kappa_y)}. \quad (40)$$

The flow pattern also decreases in eccentricity with  $\xi$  until, at high circular forcing, we recover the circularly symmetric distribution described by Eq. 33.

The rate at which work is done on the system is

$$\left\langle \frac{dW}{dt} \right\rangle = \frac{1}{2\pi} \int (\mathbf{f} \cdot \mathbf{v})_\omega d\omega \quad (41)$$

where  $(\mathbf{f} \cdot \mathbf{v})_\omega$  is a spectral density. In terms of Fourier transforms,

$$\begin{aligned} \mathbf{f}_\omega \cdot \mathbf{v}_\omega^* &= i\omega \xi \begin{bmatrix} x_\omega \\ y_\omega \end{bmatrix}^\top \begin{bmatrix} 0 & 1 \\ -1 & 0 \end{bmatrix} \begin{bmatrix} x_\omega^* \\ y_\omega^* \end{bmatrix} \\ &= i\omega \xi (x_\omega y_\omega^* - y_\omega x_\omega^*) \\ &= -2\xi \omega \operatorname{Im} x_\omega y_\omega^* \end{aligned} \quad (42)$$

from which we infer the spectral density

$$(\mathbf{f} \cdot \mathbf{v})_\omega = -2\xi \omega \operatorname{Im} (xy)_\omega. \quad (43)$$

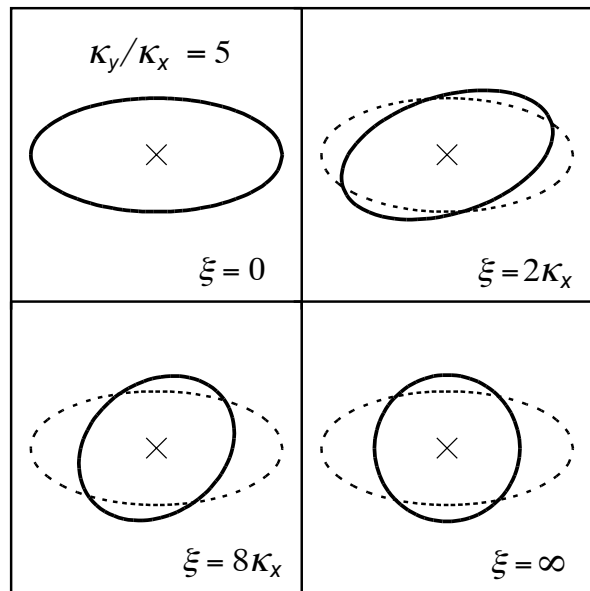


FIG. 3: R.m.s. radius  $\langle r^2 \rangle^{1/2}$  (solid curves) of the position distribution  $P(x, y)$  of a diffusing particle in a trap with stiffness anisotropy  $\kappa_y/\kappa_x = 5$ , for various values  $\xi$  of counter-clockwise circular forcing in the  $xy$  plane. The solid curves are lines of flow which, for  $\xi \neq 0$ , do not follow the  $\xi = 0$  equipotential contour (dotted curves). Circular flow at  $\xi = \infty$  (final panel, solid curve) has the r.m.s. radius  $[2k_B T / (\kappa_x + \kappa_y)]^{1/2}$ .

Using Eq. (35) for the right-hand side and performing the integral in Eq. (41) gives

$$\left\langle \frac{dW}{dt} \right\rangle = \frac{4k_B T \xi^2}{\kappa_x + \kappa_y}. \quad (44)$$

We find that the rate of work dissipated in the system by the circular nonconservative force is directly proportional to temperature, reflecting the enhancement of induced drift velocities by thermal spreading from the zero-force point. In contrast, nonconservative toroidal circulation due to axial radiation pressure [3, 4] leads to a squared dependence on temperature. Depending on the rate of outward heat flow from the optical focus [16] the proportionality of dissipation to temperature raises the possibility of an instability towards runaway heating by a nonconservative component of the trapping force.

## SUMMARY

We have characterized the simplest 3D nonconservative force field, near a stable fixed point, as an anisotropic conservative force plus a nonconservative circular force. We constructed a simple trapping model exhibiting such forcing, and presented signatures of particle displacement and nonconservative dissipation in the presence of non-conservative forcing. In most optical trapping experiments, simple circular forcing about a stationary point

may not be easily observable given the more dominant radiation pressure effects that have been observed by others [3, 4]. Specifically designing chiral trapping geometries for particles and minimizing reflections may allow observation of circular forcing. More generally, however, the geometrical picture we have constructed and the thermal and spectral results we have obtained may be useful in other situations, even outside of optics, where locally nonconservative microscopic forces act.

### Acknowledgements

The authors would like to thank their colleagues in the Department of Physics and Astronomy at Washington State University for support and helpful conversations.

- 
- [1] A. Ashkin, "Forces of a single-beam gradient laser trap on a dielectric sphere in the ray optics regime," *Biophys. J.* **61**, 569-582 (1992).
- [2] W. K. H. Panofsky and M. Phillips, *Classical Electricity and Magnetism*, 2nd Edition (Addison-Wesley, 1962).
- [3] Y. Roichman, B. Sun, A. Stolarski, and D. G. Grier, "Influence of nonconservative optical forces on the dynamics of optically trapped colloidal spheres: The fountain of probability," *Phys. Rev. Lett.* **101**, 128301-128304 (2008).
- [4] B. Sun, J. Lin, E. Darby, A. Y. Grosberg, and D. G. Grier, "Brownian vortexes," *Phys. Rev. E* **80**, 010401-010404 (2009).
- [5] S. H. Simpson and S. Hanna, "First-order nonconservative motion of optically trapped nonspherical particles," *Phys. Rev. E* **82**, 031141-031150 (2010).
- [6] D. G. B. Edelen, *Applied Exterior Calculus* (Wiley, 1985).
- [7] W. L. Burke, *Applied Differential Geometry* (Cambridge University, 1985).
- [8] T. Frankel, *The Geometry of Physics*, 2nd Edition (Cambridge University, 2004).
- [9] D. W. Jordan and P. Smith, *Nonlinear Ordinary Differential Equations*, 2nd Edition (Oxford University, 1987).
- [10] G. B. Burch, *Matrix methods in optics* (Wiley, 1975).
- [11] P. Nelson, *Biological Physics: Energy, Information, Life* (Freeman, 2008).
- [12] L. D. Landau and E. M. Lifshitz, *Statistical Physics*, 3rd Edition Part 1 (Pergamon, 1980).
- [13] F. Gittes and C. F. Schmidt, "Thermal noise limitations on micromechanical experiments," *Euro. Biophys. J.* **27**, 75-81 (1998).
- [14] K. Berg-Sørensen and H. Flyvbjerg, "Power spectrum analysis for optical tweezers" *Rev. Sci. Instr.* **75**, 594-612 (2004).
- [15] F. Gittes, B. Schnurr, P. D. Olmsted, F. C. MacKintosh, and C. F. Schmidt, "Microscopic vis-coelasticity: shear moduli of soft materials determined from thermal fluctuations," *Phys. Rev. Lett.* **79**, 3286-3289 (1997).
- [16] E. J. G. Peterman, F. Gittes, and C. F. Schmidt, "Laser-induced heating in optical traps," *Biophys. J.* **84**, 1308-1316 (2003).